Mass transfer during drop impact on a thin film: supplemental material

August 22, 2024

1 Comparison with ?

We estimated the fractional composition of secondary droplets V_{frac} from our simulations in order to compare with the experimental measurements in **?**. While our simulation are axisymmetric and so do not produce secondary droplets, the corolla nonetheless develops a bulge at its leading edge like that seen to fragment into droplets in experiments. Thus, we measured the fractional composition of the bulge, defined as the leading edge of corolla back to where the corolla has a neck (see Fig. **??**), as a stand-in for the droplet composition. **?** measurements were at $\text{Re} = 9600, \text{We} = 427, h = 0.2$. Our closest viable parameter set was at $\text{Re} = 2042$, $\text{We} = 500$, $h = 0.2$ at which $V_{\text{frac}} = 0.23$ for $t = 0.5$ and is within the observed range by **?** (Fig. 14). $\text{Re} = 3000$, $\text{We} = 500$, $h = 0.2$ is closer but it displayed bumping and so was discarded. We choose $t = 0.5$ for the comparison because after $t = 0.5$ the rate of change of V_c is small (eg from $t = 0.5$ to $t = 0.6$ the changes is less than 5%).

2 Comparison with ?

We compared the results of our simulation with the theory of **?** at $h = 0.05$ for $\text{We} = 292, \text{Re} = 1000$ & 2042 and $\text{We} = 500, \text{Re} = 1000$ & 2042. **?** predict the horizontal distance of the crown base from the impact center

$$r_c = \sqrt{2A(t - t_o)},$$

the corolla height

$$l_c = 2\sqrt{2A}\left[\sqrt{t - t_o} - \frac{1}{\sqrt{B}} \arctan\sqrt{B(t - t_o)}\right],$$

and the volume of film fluid in the corolla

$$V_c = \pi r_c^2 \left(h - h_f\right) \tag{S1}$$

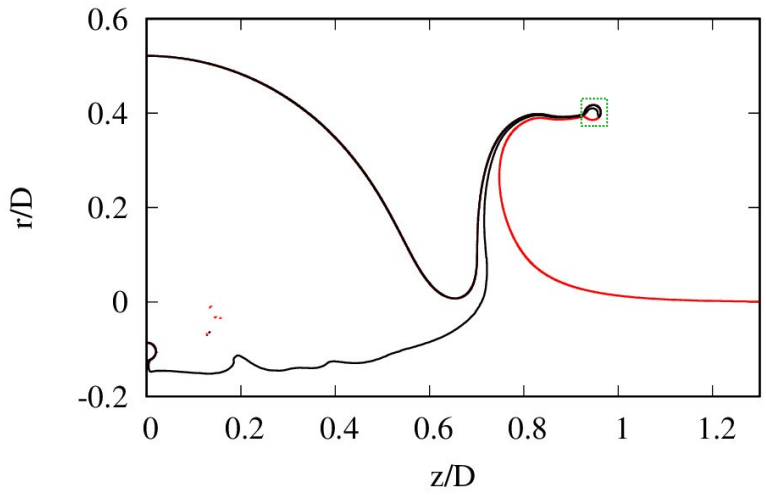

Fig. S1: Green dashed box indicates the bulge at the tip of the corolla from which V_{frac} was computed.

where h_f is the time-dependent film thickness inside the corolla

$$h_f = \frac{h}{[1 + B(t - t_0)]^2},$$

and A, B, and t_o are adjustable parameters. All equations are written in dimensionless units where lengths are scaled by D and times by D/U.

We extracted the adjustable parameters by fitting l_c versus t measured in our simulations with (i) $B = 16$ as suggested in Fig. 9 of **?** and (ii) B as a fitting parameter. Thereafter, we compared V_c as measured in simulations with Eq. **??**. Figure **??** shows the result of the fit to l_c on the left and the prediction for V_c on the right. These results demonstrate good agreement of the theory with our simulations.

3 Shape of the interface at various Weber and Reynolds numbers

The main result of this work is a map of the location of the fluid prior to impact that later goes on to form the corolla. We showed that these maps are surprisingly robust to changes in the Weber and Reynolds number. It is reasonable to wonder if perhaps the weak dependence is because the flows are also weakly dependent on We and Re. This is not the case. Figure **??** shows the range of interface shapes as We and Re are varied at fixed depth $h = 0.025$.

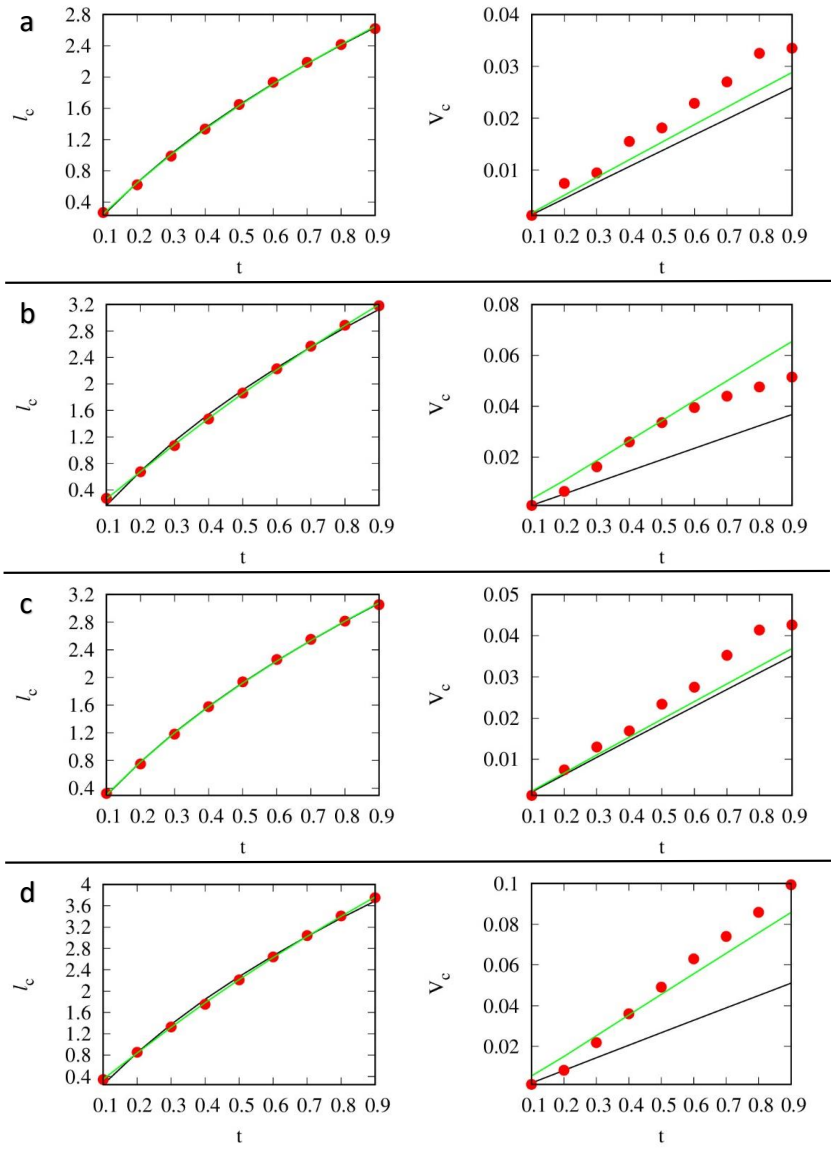

Fig. S2: Comparison of corolla sheet height and volume of the film entrained into the corolla versus time for $h = 0.05$. The simulation data is shown with circles and the two theory lines with $B = 16$ in black and B treated as a fitting parameter in green. (a) (We $=$ $292, \mathrm{Re} = 1000$) with ($A = 0.096, B = 16, t_0 = 0.19$) and ($A = 0.11, B = 13, t_0 = 0.15$). (b) (We $= 500, \mathrm{Re} = 1000$) with ($A = 0.14, B = 16, t_0 = 0.30$) and ($A = 0.24, B = 5.7, t_0 = 0.065$), (c) (We $= 292, \mathrm{Re} = 2042$) with ($A = 0.13, B = 16, t_0 = 0.17$) and ($A = 0.14, B = 14, t_0 = 0.14$), (d) (We $= 500, \mathrm{Re} = 2042$) with ($A = 0.19, t_0 = 0.26$) and ($A = 0.31, B = 6.2, t_0 = 0.035$).

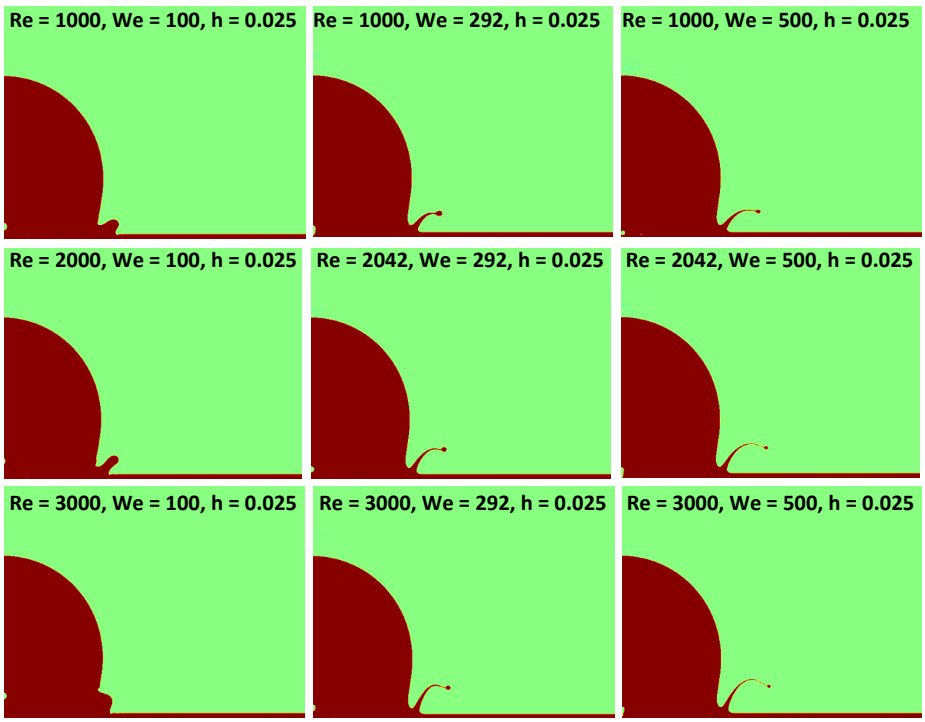

Fig. S3: Shape of the interface at $t = 0.2$ for fixed depth $h = 0.025$ and varying Re and We.

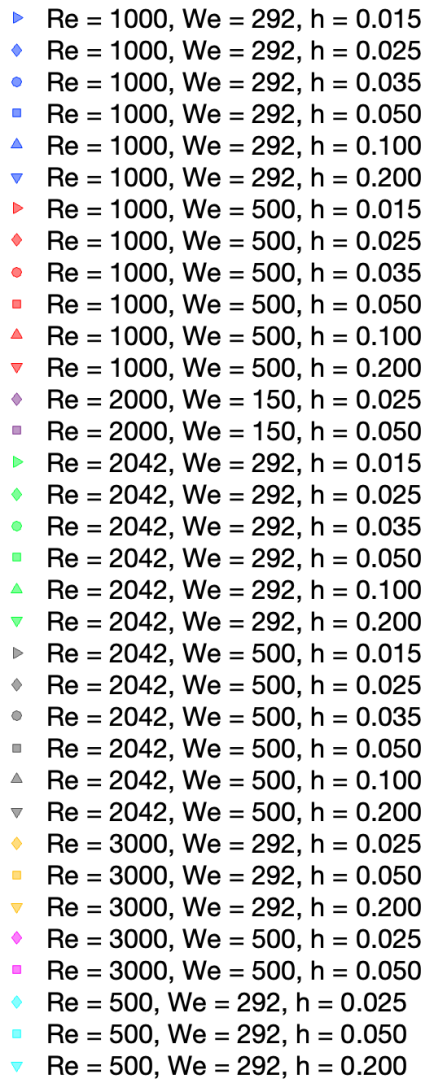

Fig. S4: Legend for Figs. 8, 9 , 10, 11 , 15